Biochemical Journal (2019) **476** 3521–3532
https://doi.org/10.1042/BCJ20190688

PORTLAND PRESS

Research Article

Arabidopsis *4-COUMAROYL-COA LIGASE 8* contributes to the biosynthesis of the benzenoid ring of coenzyme Q in peroxisomes

Eric Soubeyrand[1], Megan Kelly[1], Shea A. Keene[2], Ann C. Bernert[1], Scott Latimer[1], Timothy S. Johnson[2], Christian Elowsky[4], Thomas A. Colquhoun[2], Anna K. Block[3] and Gilles J. Basset[1]

[1]Department of Horticultural Sciences, University of Florida, Gainesville, Florida 32611, U.S.A.; [2]Department of Environmental Horticulture, Plant Innovation Center, Institute of Food and Agricultural Sciences, University of Florida, Gainesville, Florida 32611, U.S.A.; [3]Center for Medical, Agricultural and Veterinary Entomology, ARS, USDA, Gainesville, Florida 32608, U.S.A.; [4]Center for Plant Science Innovation, University of Nebraska, Lincoln, NE 68588, U.S.A.

Correspondence: Gilles J. Basset (gbasset@ufl.edu)

Plants have evolved the ability to derive the benzenoid moiety of the respiratory cofactor and antioxidant, ubiquinone (coenzyme Q), either from the β-oxidative metabolism of *p*-coumarate or from the peroxidative cleavage of kaempferol. Here, isotopic feeding assays, gene co-expression analysis and reverse genetics identified Arabidopsis *4-COUMARATE-COA LIGASE 8* (*4-CL8*; *At5g38120*) as a contributor to the β-oxidation of *p*-coumarate for ubiquinone biosynthesis. The enzyme is part of the same clade (V) of acyl-activating enzymes than At4g19010, a *p*-coumarate CoA ligase known to play a central role in the conversion of *p*-coumarate into 4-hydroxybenzoate. A *4-cl8* T-DNA knockout displayed a 20% decrease in ubiquinone content compared with wild-type plants, while 4-CL8 overexpression boosted ubiquinone content up to 150% of the control level. Similarly, the isotopic enrichment of ubiquinone's ring was decreased by 28% in the *4-cl8* knockout as compared with wild-type controls when Phe-[*Ring*-$^{13}C_6$] was fed to the plants. This metabolic blockage could be bypassed via the exogenous supply of 4-hydroxybenzoate, the product of *p*-coumarate β-oxidation. Arabidopsis 4-CL8 displays a canonical peroxisomal targeting sequence type 1, and confocal microscopy experiments using fused fluorescent reporters demonstrated that this enzyme is imported into peroxisomes. Time course feeding assays using Phe-[*Ring*-$^{13}C_6$] in a series of Arabidopsis single and double knockouts blocked in the β-oxidative metabolism of *p*-coumarate (*4-cl8; at4g19010; at4g19010 × 4-cl8)*, flavonol biosynthesis (*flavanone-3-hydroxylase*), or both (*at4g19010 × flavanone-3-hydroxylase*) indicated that continuous high light treatments (500 μE m^{-2} s^{-1}; 24 h) markedly stimulated the *de novo* biosynthesis of ubiquinone independently of kaempferol catabolism.

Introduction

Ubiquinone (Coenzyme Q) is a liposoluble redox cofactor that is essential for energy metabolism and membrane protection in eukaryotes and numerous bacterial species [1,2]. The core function of ubiquinone is to serve in the respiratory chain as the mobile electron carrier between Complex I (NADH dehydrogenase) or Complex II (succinate dehydrogenase) and Complex III (cytochrome c reductase). Alternative NAD(P)H dehydrogenases and other oxidoreductases also use ubiquinone to feed electrons directly into the respiratory chain; plant genomes, in particular, encode an atypically high number of such ubiquinone-dependent enzymes, which are important for photorespiration, redox balancing, and the catabolism of lysine and branched-chain amino acids [3,4]. Besides its role in energy metabolism, ubiquinone doubles as a crucial free-radical scavenger that protects lipids and integral membrane proteins from oxidative damage. For instance, yeast mutants that lack ubiquinone

Accepted Manuscript online: 5 November 2019
Version of Record published: 27 November 2019

Biochemical Journal (2019) **476** 3521–3532
https://doi.org/10.1042/BCJ20190688

PORTLAND PRESS

Research Article

Arabidopsis *4-COUMAROYL-COA LIGASE 8* contributes to the biosynthesis of the benzenoid ring of coenzyme Q in peroxisomes

Eric Soubeyrand[1], Megan Kelly[1], Shea A. Keene[2], Ann C. Bernert[1], Scott Latimer[1], Timothy S. Johnson[2], Christian Elowsky[4], Thomas A. Colquhoun[2], Anna K. Block[3] and Gilles J. Basset[1]

[1]Department of Horticultural Sciences, University of Florida, Gainesville, Florida 32611, U.S.A.; [2]Department of Environmental Horticulture, Plant Innovation Center, Institute of Food and Agricultural Sciences, University of Florida, Gainesville, Florida 32611, U.S.A.; [3]Center for Medical, Agricultural and Veterinary Entomology, ARS, USDA, Gainesville, Florida 32608, U.S.A.; [4]Center for Plant Science Innovation, University of Nebraska, Lincoln, NE 68588, U.S.A.

Correspondence: Gilles J. Basset (gbasset@ufl.edu)

Plants have evolved the ability to derive the benzenoid moiety of the respiratory cofactor and antioxidant, ubiquinone (coenzyme Q), either from the β-oxidative metabolism of *p*-coumarate or from the peroxidative cleavage of kaempferol. Here, isotopic feeding assays, gene co-expression analysis and reverse genetics identified Arabidopsis *4-COUMARATE-COA LIGASE 8* (*4-CL8*; *At5g38120*) as a contributor to the β-oxidation of *p*-coumarate for ubiquinone biosynthesis. The enzyme is part of the same clade (V) of acyl-activating enzymes than At4g19010, a *p*-coumarate CoA ligase known to play a central role in the conversion of *p*-coumarate into 4-hydroxybenzoate. A *4-cl8* T-DNA knockout displayed a 20% decrease in ubiquinone content compared with wild-type plants, while 4-CL8 overexpression boosted ubiquinone content up to 150% of the control level. Similarly, the isotopic enrichment of ubiquinone's ring was decreased by 28% in the *4-cl8* knockout as compared with wild-type controls when Phe-[*Ring*-$^{13}C_6$] was fed to the plants. This metabolic blockage could be bypassed via the exogenous supply of 4-hydroxybenzoate, the product of *p*-coumarate β-oxidation. Arabidopsis 4-CL8 displays a canonical peroxisomal targeting sequence type 1, and confocal microscopy experiments using fused fluorescent reporters demonstrated that this enzyme is imported into peroxisomes. Time course feeding assays using Phe-[*Ring*-$^{13}C_6$] in a series of Arabidopsis single and double knockouts blocked in the β-oxidative metabolism of *p*-coumarate (*4-cl8; at4g19010; at4g19010 × 4-cl8)*, flavonol biosynthesis (*flavanone-3-hydroxylase*), or both (*at4g19010 × flavanone-3-hydroxylase*) indicated that continuous high light treatments (500 μE m^{-2} s^{-1}; 24 h) markedly stimulated the *de novo* biosynthesis of ubiquinone independently of kaempferol catabolism.

Introduction

Ubiquinone (Coenzyme Q) is a liposoluble redox cofactor that is essential for energy metabolism and membrane protection in eukaryotes and numerous bacterial species [1,2]. The core function of ubiquinone is to serve in the respiratory chain as the mobile electron carrier between Complex I (NADH dehydrogenase) or Complex II (succinate dehydrogenase) and Complex III (cytochrome c reductase). Alternative NAD(P)H dehydrogenases and other oxidoreductases also use ubiquinone to feed electrons directly into the respiratory chain; plant genomes, in particular, encode an atypically high number of such ubiquinone-dependent enzymes, which are important for photorespiration, redox balancing, and the catabolism of lysine and branched-chain amino acids [3,4]. Besides its role in energy metabolism, ubiquinone doubles as a crucial free-radical scavenger that protects lipids and integral membrane proteins from oxidative damage. For instance, yeast mutants that lack ubiquinone

Accepted Manuscript online: 5 November 2019
Version of Record published: 27 November 2019

Biochemical Journal (2019) 476 3521–3532
https://doi.org/10.1042/BCJ20190688

display a pronounced decrease in viability when exposed to peroxyl radicals, while plant transgenics that contain enhanced levels of ubiquinone are more resistant to oxidative stress [5–7]. Reflecting the vital roles of ubiquinone, mutations that abolish ubiquinone biosynthesis in plants result in embryo lethality [8,9].

Living organisms synthesize ubiquinone from the prenylation of an aromatic precursor, which is then further decorated with methoxy, hydroxyl and methyl groups (Figure 1). In most cases, the aromatic precursor is 4-hydroxybenzoate (Figure 1). Plants are unique in having evolved the ability to synthesize this precursor via two parallel branches of phenylpropanoid metabolism. In the first branch, *p*-coumarate is imported into peroxisomes, where its propyl chain is β-oxidized leading to the formation of 4-hydroxybenzoate (Figure 1). Loss of function of either the Arabidopsis *PEROXISOMAL ABC TRANSPORTER 1* (*PXA1*), which is crucial for the import of *p*-coumarate into peroxisomes (Figure 1), or the peroxisomal *p*-coumaroyl-CoA ligase product of gene *at4g19010*, which is involved in the activation of the propyl moiety of *p*-coumarate (Figure 1), results in a decrease in ubiquinone content of ∼60% [10], suggesting that the β-oxidative metabolism of *p*-coumarate is the predominant route for the supply of ubiquinone's ring in Arabidopsis. In the second branch of 4-hydroxybenzoate formation from phenylpropanoids, *p*-coumarate enters flavonoid biosynthesis, eventually forming the hydroxyphenyl moiety (i.e. B-ring) of kaempferol. The latter can then serve as a substrate for some peroxidases that cleave the B-ring, generating 4-hydroxybenzoate as a product [11] (Figure 1). Blockage of the biosynthesis of kaempferol, for instance via knocking out *flavanone-3-hydroxylase* (*f3h*) or the genes encoding for some upstream enzymes, such as *4-COUMAROYL-COA LIGASE 3* (*4-CL3*) and *CHALCONE SYNTHASE* (*CHS*), indicated that this

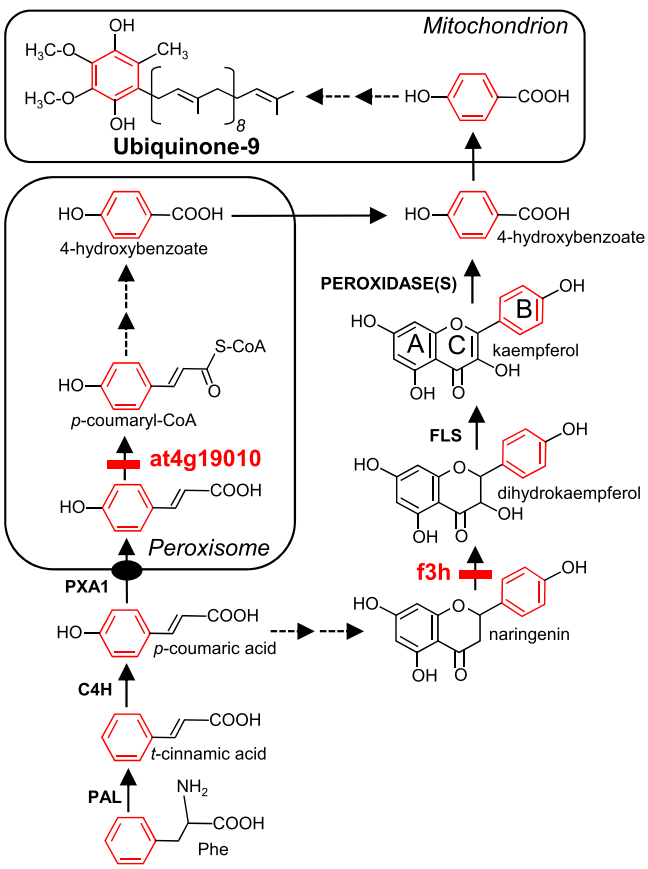

Figure 1. Overview of the architecture of 4-hydroxybenzoate biosynthesis for use as a precursor of ubiquinone's benzenoid moiety in plant cells.The red bars indicate the locations of the metabolic blockages resulting from the loss of function of *p*-coumaroyl-CoA ligase (at4g19010) and of flavanone-3-hydroxylase (f3h) in the peroxisomal and cytosolic branches of 4-hydroxybenzoate formation from Phe, respectively. C4H, cinnamate-4-hydroxylase; AT4G19010, peroxisomal *p*-coumaroyl-CoA ligase; F3H, flavanone-3-hydroxylase; FLS, flavonol synthase; PAL, phenylalanine ammonia lyase; PXA1, peroxisomal ABC transporter 1. Dashed arrows indicate multiple steps.

Biochemical Journal (2019) 476 3521–3532
https://doi.org/10.1042/BCJ20190688

cytosolic route of 4-hydroxybenzoate formation contributes to ∼20% of ubiquinone formation in Arabidopsis [11]. The 4-hydroxybenzoate originating either from the β-oxidative metabolism of *p*-coumarate or from the peroxidative cleavage of kaempferol is then imported into mitochondria, where the reactions of prenylation, decarboxylation, hydroxylation, and methylation take place (Figure 1). Furthermore, as in other eukaryotes, tyrosine can serve in plants as a ring precursor of ubiquinone [10]. Although none of the cognate enzymes are known in plants, it has been shown that this alternative route is distinct from phenylpropanoid metabolism [10]. The existence of such a parallel source of ring precursor stemming from tyrosine is crucial for the genetic dissection of ubiquinone biosynthesis in plants, as it permits the isolation of viable mutants in the phenylpropanoid route.

In this study, we sought to investigate whether there existed some additional functional redundancies in the biosynthesis of 4-hydroxybenzoate from phenylpropanoids. To do that, we generated an Arabidopsis double knockout that was predicted to block both the β-oxidative and flavonoid branches of 4-hydroxybenzoate biosynthesis. Having shown that this double mutant was able to maintain a basal incorporation of ^{13}C-labelled phenylalanine into ubiquinone, we identified an additional *p*-coumaroyl-CoA ligase involved in the β-oxidative metabolism of *p*-coumarate. Furthermore, because plant exposure to high light is known to markedly stimulate flavonoid biosynthesis, we explored the question of whether the respective contributions of the peroxisomal and cytosolic routes of 4-hydroxybenzoate biosynthesis were dependent upon the light regime.

Experimental

Chemicals and reagents

Ubiquinone-9 and ubiquinone-10 standards were from Sigma–Aldrich and were quantified spectrophotometrically in 100% ethanol using the extinction coefficient of 14 700 M^{-1} cm^{-1} and of 14 700 M^{-1} cm^{-1} at 275 nm, respectively [12]. Their corresponding reduced forms (quinols) were prepared by reaction with sodium borohydride. L-phenylalanine-[*ring*-$^{13}C_6$] and L-tyrosine-[*ring*-$^{13}C_9$-^{15}N] were from Cambridge Isotope Laboratories Inc. Murashige and Skoog medium was from MP Biomedicals, LLC. Unless otherwise mentioned, other chemicals and reagents were from Fisher Scientific. All PCR-generated constructs were verified by sequencing.

Plant material and growth conditions

Arabidopsis T-DNA insertion lines *4cl8-1* (SALK_137753) and *4cl8-2* (SALK_148185) were obtained from the Arabidopsis Biological Resource Center [13]. The knockout mutants corresponding to *at4g19010* (SALK_043310) and *f3h* (SALK_113321) were those described and confirmed as null alleles in [10] and [14], respectively. Plants were grown in a plug and germination soil mix at 22°C, 12-h days (160 μE m^{-2} s^{-1}) using standard fertilization treatments. For ^{13}C tracer experiments and chemical rescue assays, Arabidopsis seeds were germinated on Murashige and Skoog agar plates supplemented with 1% (w/v) sucrose. After 7 days, seedlings were transferred to 250 ml flasks containing 20 ml of Murashige and Skoog medium supplemented with 1% (w/v) sucrose on an orbital shaker (60 rpm) at 22°C in 10-h days (160 μE m^{-2} s^{-1}). For dark and high light treatments, plants were acclimated to continuous darkness or continuous high light intensity (500 μE m^{-2} s^{-1}) for 24 h prior to feeding with L-phenylalanine-[*ring*-$^{13}C_6$].

Genotyping and RT-PCR analyses

Arabidopsis *4-Cl8* insertion lines were PCR-genotyped using GoTaq polymerase (Promega) and T-DNA specific primer LBb1 5′-GCGTGGACCGCTTGCTGCAACTT-3′ in combination with line specific primers: LP 5′-GTGGAGGAGAGTCGGAGGTAC-3′ and RP 5′-TGCATGGCTTTGATCATTAAAG-3′ for SALK_137753, and LP 5′-TCGAAACAATAATTTCTTCAATCG-3′ and RP 5′-ACCTCCAGCTGAACTAGAGGC-3′ for SALK_148185. Total leaf RNA were extracted using the RNAeasy Plant Mini Kit (Qiagen), and RT-PCR were performed on 1 μg of RNAs using the following gene specific primers: RTfwd 5′-GCCACCTTAGCGTTAGGTACG-3′) and RTrev 5′-CTGGAAACGGAATAACGGCT-3′ for *4-CL8*, and RTfwd 5′-CTAAGCTCTCAAGATCAAAGGC-3′ and RTrev 5′-TTAACATTGCAAAGAGTTTCAAGG-3′ for the actin control.

Functional complementation of the *4-cl8* knockout and subcellular localization

Full-length *4-CL8* cDNA was PCR-amplified using Phusion polymerase with the primer pair 4-CL8fwd 5′-CACCATGGCGAATTCTCAAAGATCATCATCTCTGATCG-3′ and 4-CL8rev 5′-TTAAATTTTTGAAATGGCAAATTTGATTAGATCCTTGCG-3′; the resulting fragment was subcloned into pENTR/D-TOPO (Invitrogen). For complementation of the *4-cl8* knockout, the 4-CL8 cDNA was transferred from pENTR/D-TOPO

Biochemical Journal (2019) 476 3521–3532
https://doi.org/10.1042/BCJ20190688

(Invitrogen) into pB2GW7 [15] using Gateway technology. This construct was introduced into SALK_137753 line via *Agrobacterium tumefaciens* using the floral dip method [16]. The transformants were selected on soil with glufosinate sprays (120 mg L^{-1}). For subcellular localization experiments, the *4-CL8* cDNA was transferred from pENTR/D-TOPO into pK7WGF2 (Karimi et al. [15]) using Gateway technology, resulting in an in-frame fusion of the 5′-end of *4-CL8* to the 3′-end of the green fluorescent protein (GFP) DNA. Construct PZP212-KAT2-eqFP611 served as a fluorescent reporter of peroxisomes [10]. The pK7WGF2T-*4-Cl8* and PZP212-KAT2-eqFP611 constructs were separately electroporated into *A. tumefaciens* for subsequent coinfiltration into the abaxial side leaves of *Nicotiana benthamiana*. Epidermal cells were imaged 48 h later on detached leaves using a Nikon A1 laser scanning confocal microscope on a Nikon 90i compound microscope with a Plan Apo VC60x WI DIC N2 objective. Data acquisition and image analysis was with NIS-Element 4.40.00. GFP, RFP, and chlorophyll were excited and collected sequentially using the following excitation/emissions wavelengths: 488 nm/500–550 nm for GFP, 561 nm/570–620 nm for RFP, and 641 nm/663–738 nm for chlorophyll.

Ubiquinone analyses

Arabidopsis leaves (50–100 mg of fresh weight) or flower buds (20–40 mg of fresh weight) were spiked with 3.5–7 nmoles (spectrophotometric detection) or 70 pmoles (mass spectrometry detection) of an internal standard of ubiquinone-10, and ground using a 5-ml Pyrex tissue grinder in 0.4 ml of 95% (v/v) ethanol. The extract was transferred to a 10-ml pyrex screw-cap tube containing 0.5 ml of water and the grinder was washed twice with 0.3 ml of 95% (v/v) ethanol, each time combining the washes to the initial extract. This mixture was then partitioned twice with 5 ml hexane, the hexane layers were combined, and evaporated to dryness with gaseous nitrogen. Samples were either resuspended in 0.2 ml of methanol : dichloromethane (10 : 1, v/v) and analyzed immediately, or stored desiccated at −20°C for further analysis. Pilot experiments showed no statistically significant difference in ubiquinone content between samples analyzed immediately or those stored at −20°C for up to 2 months. For the determination of total ubiquinone-9 content in leaves and flower buds using HPLC-diode array spectrophotometry, resuspended extracts (0.2 ml) were reduced with 40 µl of 200 mM $NaBH_4$ prepared in 100% ethanol. Samples were then centrifuged (5 min; 21 000×***g***) and immediately injected on a 5 µM Supelco Discovery C-18 column (250 × 4.6 mm) thermostated at 30°C and developed in isocratic mode at a flow rate of 1 ml min^{-1} with methanol : hexane (90 : 10, v/v). Ubiquinol-9 (9.7 min) and ubiquinol-10 (12.3 min) were monitored at 290 nm; ubiquinone-10 (17.4 min) was monitored at 275 nm. Quinols and quinones were quantified according to their respective external standards, and ubiquinone-9 amounts were corrected for recovery (>70%) and re-oxidation (<10%) of the ubiquinone-10 internal standard. For analysis by liquid chromatography-electrospray ionization-tandem mass spectrometry, 5 µl of the extracts resuspended in methanol : dichloromethane (10 : 1, v/v) were chromatographed on a Zorbax SB-C18 rapid resolution HT column (50 mm × 2.1 mm; 1.8 µm; Agilent Technologies) held at 40°C and developed isocratically with 5 mM ammonium formate in 100% methanol at a flow rate of 0.4 ml min^{-1}. The eluate was electrosprayed in positive mode with a nitrogen gas temperature of 300°C at a flow rate of 10 L min^{-1} into an Agilent 6430 Triple Quadrupole mass spectrometer. Nebulizer pressure was 35 psi and capillary potential voltage was set to 4000 V. Quinols and quinones were analyzed by multiple reaction monitoring using dwell time of 50 ms and the following ion pairs: ubiquinol-9 (814.6/197) and [$^{13}C_6$ *ring*]-ubiquinol-9 (820.6/203) at 3.94 min, ubiquinol-10 (882.7/197) and [$^{13}C_6$ *ring*]-ubiquinol-10 (888.7/203) at 6.46 min, ubiquinone-9 (812.6/197) and [$^{13}C_6$ *ring*]-ubiquinone-9 (818.6/203) at 7.98 min, ubiquinone-10 (880.7/197) and [$^{13}C_6$ *ring*]-ubiquinone-10 (886.7/203) at 13.72 min.

Results

The *at4g19010* × *f3h* double knockout can still synthesize ubiquinone from phenylalanine

To test the effect of disabling both the peroxisomal and cytosolic branches leading to the formation of ubiquinone's ring from phenylalanine, a cognate Arabidopsis double knockout was generated by crossing the *at4g19010* and *f3h* T-DNA knockout lines (Figure 1). Genotyping of the progeny of double heterozygote plants indicated that segregation ratios were typical of the expected value for two unlinked alleles, and that the double knockout plants were phenotypically indistinguishable from their wild-type and single knockout counterparts (Supplementary Table S1 and Supplementary Fig. S1). Furthermore, HPLC analysis of wild-type, *f3h*, *at4g19010* and *at4g19010* × *f3h* leaf extracts showed that the simultaneous blockage of the peroxisomal and cytosolic sources of 4-hydroxybenzoate did not result in any additive effect on total ubiquinone content (Figure 2a).

Biochemical Journal (2019) **476** 3521–3532
https://doi.org/10.1042/BCJ20190688

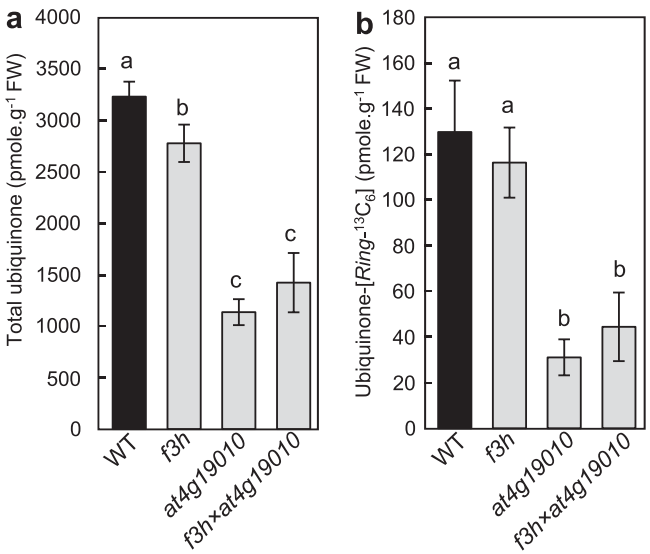

Figure 2. Ubiquinone levels and isotopic feeding assays in Arabidopsis.

(**a**) Total ubiquinone (reduced and oxidized) content in the leaves of axenically grown *f3h, at4g19010* and *f3h* × *at4g19010* knockout plants and their wild-type reference. (**b**) *De novo* biosynthesis of ubiquinone-[*Ring*-$^{13}C_6$] in axenically grown wild-type, *f3h*, *at4g19010* and *f3h* × *at4g19010* Arabidopsis plants fed for 3 h with 250 μM doses of Phe-[*Ring*-$^{13}C_6$]. Values are means of four biological replicates ± S.E. Different letters indicate statistically significant differences as calculated by Tukey's test ($P < 0.05$).

Quantification of *de novo* ubiquinone biosynthesis by liquid chromatography-tandem mass spectrometry in corresponding seedlings axenically fed for 3 h with identical doses of Phe-[*Ring*-$^{13}C_6$] recapitulated these results (Figure 2b). The isotopic enrichments of ubiquinone-[*Ring*-$^{13}C_6$] were decreased by ∼70% and 20% as compared with the wild type in the *at4g19010* and *f3h* knockouts, respectively, but here again no statistically significant differences were observed between *at4g19010* and *at4g19010* × *f3h* knockout plants (Figure 2b).

These data show that despite the simultaneous blockage of the biosynthesis of 4-hydroxybenzoate in peroxisomes and in the cytosol, the *at4g19010* × *f3h* knockout plants are still able to maintain a basal level of ubiquinone originating from phenylalanine. Since cinnamate-4-hydroxylase (Figure 1) represents the obligatory passage for the incorporation of phenylalanine into ubiquinone [11], we inferred that Arabidopsis has evolved the capacity to use *p*-coumarate for ubiquinone biosynthesis either via a third route -i.e. independently from the β-oxidation of *p*-coumarate and the peroxidative cleavage of kaempferol- or via one or more functionally redundant *p*-coumarate ligase in peroxisomes or flavanone-3-hydroxylase in the cytosol.

Arabidopsis *4-COUMARATE-COA LIGASE 8* contributes to the biosynthesis of ubiquinone from phenylalanine

The existence of missing enzymes involved in the incorporation of *p*-coumarate into ubiquinone prompted us to re-examine the co-expression networks of genes connected to ubiquinone metabolism and function. Query genes encoding for components of the mitochondrial respiratory chain, flavonoid and phenylpropanoid biosynthetic enzymes, and enzymes involved in the prenylation, hydroxylation and methylation of ubiquinone's ring were therefore used to mine the ATTED-II microarray and RNA-seq database [17]. Such searches identified *4-COUMARATE-COA LIGASE 8* (*4-CL8*; *At5g38120*) among the top 1.5% co-expressors of *FLAVONOL SYNTHASE 1* (*At5g08640*) that catalyzes the conversion of dihydrokaempferol into kaempferol, *CHALCONE SYNTHASE* (*At5g13930*), mitochondrial *ATP/PHOSPHATE CARRIER 1* (*At5g61810*), *ALTERNATIVE NAD(P)H DEHYDROGENASE 1* (*At1g07180*), which uses ubiquinone to oxidize NADH in mitochondria [18], and mitochondrial *GERANYL GERANYL PYROPHOSPHATE SYNTHASE 1* (*At1g49530*) (Supplementary data S1). It is equally remarkable that 4-CL8 belongs to the same small clade of acyl activating enzymes as At4g19010 [19]. Furthermore, like At4g19010, 4-CL8 displays a canonical C-terminal peroxisomal targeting signal type 1. We will come back to this crucial feature later.

Biochemical Journal (2019) 476 3521–3532
https://doi.org/10.1042/BCJ20190688

To examine the biological function of *4-CL8*, two T-DNA lines corresponding to predicted insertions in the second intron (SALK_137753) and in the fifth exon (SALK_148185) of *At5g38120* were identified in the SALK collection [13] and confirmed by DNA genotyping (Figure 3a,b). RT-PCR analyses in rosette leaves indicated that SALK_137753 corresponded to a genuine knockout of *At5g38120*, while SALK_148185 did not (Figure 3c). This latter line was therefore investigated no further, and three independent complemented lines consisting of the SALK_137753 knockout transformed with full-length *4-CL8* cDNA under the control of the 35S promoter were generated (Figure 3c). No phenotypic difference was observed between the *4-cl8* knockout and its wild-type reference (Supplementary Fig. S1), but ubiquinone content in the mutant was decreased by 20% as compared with that of wild-type plants (Figure 4a). In contrast, the three *4-CL8* overexpressing lines accumulated ubiquinone to 125–150% of wild-type level (Figure 4a). Similarly, when Phe-[*Ring*-$^{13}C_6$] was axenically fed to wild-type and *4-cl8* plants, the isotopic enrichment of ubiquinone's ring was decreased by 28–38% in the *4-cl8* knockout as compared with the wild-type control and the complemented lines (Figure 4b). In contrast, no statistically significant difference in the incorporation of ^{13}C into ubiquinone was measured when Tyr-[$^{13}C_9$; ^{15}N] was fed to *4-cl8* and wild-type plans cultures (Figure 4b). Also notable was the observation that feeding 4-hydroxybenzoate (the product of *p*-coumarate β-oxidation) to the *4-cl8* knockout restored ubiquinone content to wild-type level (Figure 4c). All together, these results point to 4-CL8 as an additional class V *p*-coumaroyl-CoA ligase that contributes to the biosynthesis of the ring of ubiquinone via the phenylalanine pathway.

Arabidopsis 4-COUMARATE-COA LIGASE 8 is localized in peroxisomes

One of the defining attributes of acyl-activating enzyme clade V, which contains 4-CL8, is that all its members display C-terminal tripeptides corresponding to peroxisomal targeting sequence type 1 or PTS1 [20]. In the case of 4-CL8, the functional authenticity of this targeting signal is confirmed by the strict conservation of canonical PTS1 (-SKI/-SKL/-SRL) in homologs of 4-CL8 sampled throughout Brassicaceae (Figure 5). To further verify this observation, the full-length cDNA of Arabidopsis *4-CL8* was fused in frame to the 3′-end of the green fluorescent protein (GFP), and this construct was co-infiltrated in *N. benthamiana* leaf tissues with that of a red fluorescent protein (RFP)-tagged peroxisomal marker. Laser scanning confocal imaging of epidermal cells showed that co-expression of the two constructs resulted in a distinct pattern of small punctate structures, where the fluorescence associated with GFP co-localized with that of RFP (Figure 5).

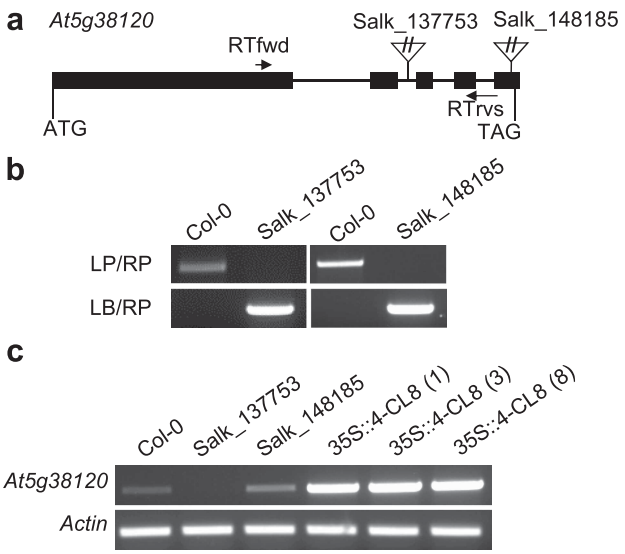

Figure 3. Molecular characterization of Arabidopsis *4-COUMARATE-COA LIGASE 8* (*At5g38120*) T-DNA insertion mutants.

(**a**) Structure of the *At5g38120* locus and location of T-DNA insertions SALK_137753 and SALK_148185. Boxes and lines represent exons and introns, respectively. (**b**) Genotyping PCR of wild-type Arabidopsis plants (Col-0) and homozygous T-DNA insertion mutants SALK_137753 and SALK_148185. RP and LP: gene specific primers; LB: T-DNA specific primer. (**c**) RT-PCR analyses of the rosette leaves of wild-type Arabidopsis plants, homozygous T-DNA insertion mutants SALK_137753 and SALK_148185 and complemented lines SALK137753-35S::At5g38120 cDNA 1, 3 and 8. Actin: RT-PCR and loading control.

Biochemical Journal (2019) **476** 3521–3532
https://doi.org/10.1042/BCJ20190688

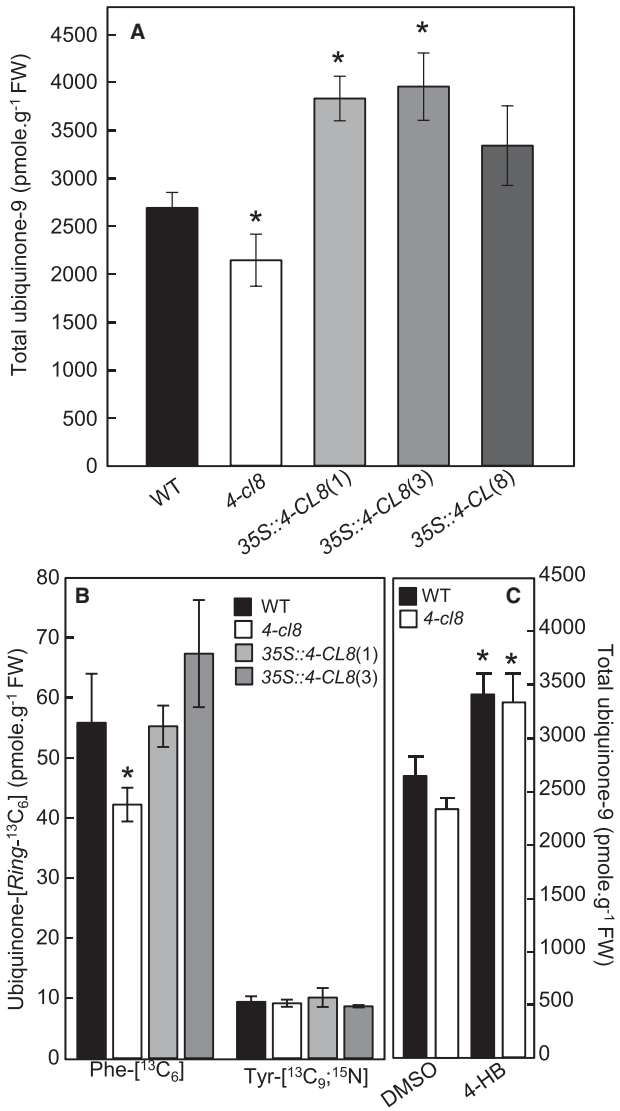

Figure 4. Arabidopsis *4-COUMARATE-COA LIGASE 8* contributes to the biosynthesis of ubiquinone from phenylalanine.
(**a**) Total ubiquinone-9 content in 4-week old rosette leaves of wild-type, *4-cl8, and* complemented *4-cl8* (35S::4-CL8 lines 1, 3, 8) Arabidopsis plants. (**b**) Ubiquinone-[*Ring*-$^{13}C_6$] content in axenically grown wild-type, *4-cl8* and complemented *4-cl8* (lines 1 and 3) Arabidopsis plants fed for 3 h with 250 μM doses of Phe-[$^{13}C_6$] or Tyr-[$^{13}C_9$;^{15}N]. (**c**) Total ubiquinone content in axenically grown wild-type and *4-cl8* knockout Arabidopsis plants fed for 24 h with 10 μM of 4-hydroxybenzoate (4-HB). Data are means of 5–10 (**a**), 4–5 (**b**), or 4 (**c**) biological replicates ± SE. Asterisks in (**a**) and (**b**) indicate significant differences as compared with wild-type control as determined by Fisher's test ($P < \alpha = 0.1$) from an analysis of variance. Asterisks in (**c**) indicate significant differences as compared with the DMSO controls as determined by Fisher's test ($P < \alpha = 0.05$) from an analysis of variance.

Different light conditions modify the contribution of At4g19010 to ubiquinone biosynthesis, but not that of 4-CL8 or the flavonoid pathway

The occurrence of functional redundancies in the biosynthesis of the ring of ubiquinone from phenylalanine invites the question of whether the cognate enzymes and biosynthetic branches are differentially regulated in response to environmental factors. This is the case in particular for the flavonoid pathway, which supplies the intermediates for anthocyanin biosynthesis and is strongly up-regulated in high light [21,22]. One could

Biochemical Journal (2019) **476** 3521–3532
https://doi.org/10.1042/BCJ20190688

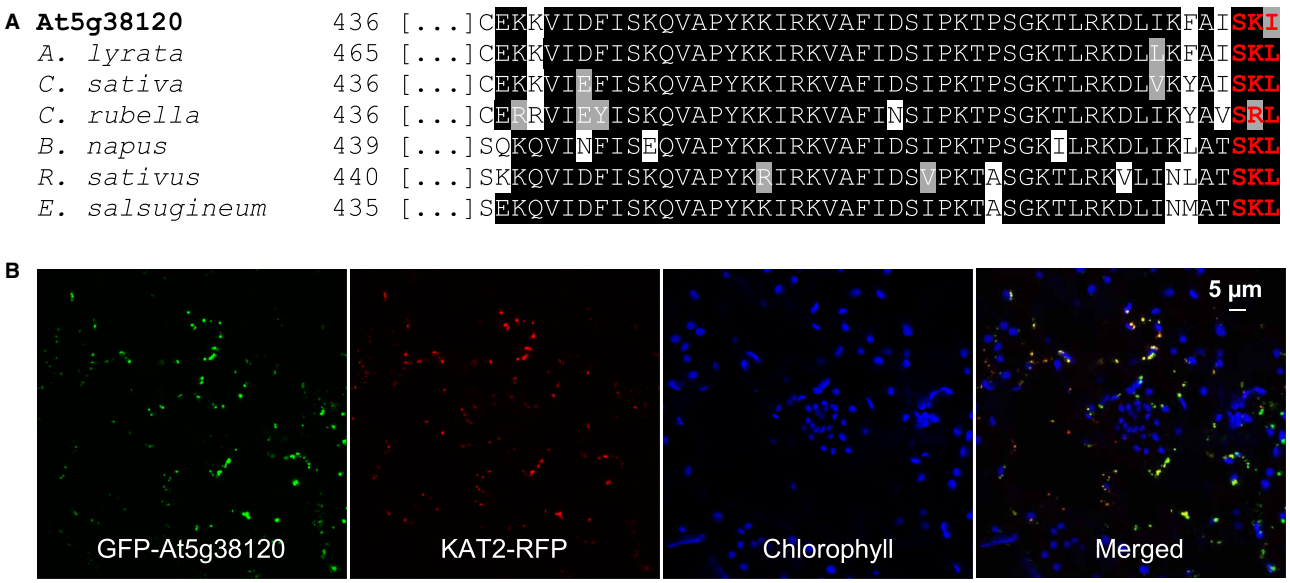

Figure 5. Subcellular localization of Arabidopsis 4-COUMARATE-COA LIGASE 8.

(**a**) Alignment of the C-terminal regions of Arabidopsis 4-COUMARATE-COA LIGASE 8 (At5g38120) and its orthologs in *Arabidopsis lyrata*, *Camelina sativa*, *Capsella rubella*, *Brassica napus*, *Raphanus sativus* and *Eutrema salsugineum*. The consensus peroxisomal targeting sequence type 1 tripeptides are highlighted in red. Identical residues are shaded in black, similar residues are shaded in grey. (**b**) Transient expression in *Nicotiana benthamiana* epidermal cells and confocal laser scanning microscopy imaging of At5g38120 fused to the C-terminus of GFP (GFP-At5g38120; green pseudocolor). KAT2-RFP (red pseudocolor), peroxisomal marker RFP-tagged 3-keto-acyl-CoA thiolase 2 co-infiltrated with GFP-At5g38120; Chlorophyll (blue pseudocolor). Merged, overlay of green, red, and blue pseudocolors.

hypothesize that in these conditions the availability of kaempferol for ubiquinone biosynthesis decreases, and therefore that the contribution of the β-oxidative branch in peroxisomes increases.

To investigate such a possibility, axenic cultures of the *f3h*, *4-cl8*, and *at4g19010* knockouts, as well as the *at4g19010* × *f3h* and *at4g19010* × *4-cl8* double knockouts and their wild-type counterparts were subjected to 24 h of either continuous dark or continuous high light treatments (500 µE m^{-2} s^{-1}). Axenic cultures grown at 14 h-dark/10h-light (160 µE m^{-2} s^{-1}) served as controls. Phenylalanine-[*Ring*-$^{13}C_6$] was then fed for 2 h and 3 h to each culture and the ^{13}C isotopic enrichment of ubiquinone was determined. High light markedly stimulated the *de novo* biosynthesis of ubiquinone of all cultures: the increase varying from 2-fold as compared with that measured in the 14 h-dark/10 h-light controls for wild-type, *f3h*, *4-cl8* plants to up to 3–5-fold in the case of the *at4g19010*, *at4g19010* × *f3h*, and *at4g19010* × *4-cl8* knockouts (Figure 6a). In contrast, when cultures were subjected to continuous dark treatment, wild-type, *f3h* and *4cl8* plants displayed a 25–35% decrease in *de novo* ubiquinone biosynthesis as compared with the 14 h-dark/10 h-light controls, while no statistically significant difference in the incorporation of phenylalanine-[*Ring*-$^{13}C_6$] into ubiquinone was detected for the *at4g19010*, *at4g19010* × *f3h*, and *at4g19010* × *4-cl8* knockouts (Figure 6a).

When compared with wild-type plants, the *de novo* biosynthesis of ubiquinone was decreased by ∼20% in the *f3h* and *4-cl8* knockouts independently of the light regime (Figure 6b). In the case of the *at4g19010*, *at4g19010* × *f3h*, and *at4g19010* × *4-cl8* knockouts, *de novo* biosynthesis of ubiquinone was decreased to ∼25% of wild-type levels in both 14 h-dark/10 h-light and continuous dark conditions, but to only 55–65% of wild-type levels when the cultures were subjected to continuous high light (Figure 6b). It thus emerges from these data that continuous high light treatments markedly stimulate the *de novo* biosynthesis of ubiquinone in Arabidopsis. Changes in light conditions, however, selectively impact some of the enzymes and biosynthetic branches involved in the formation of the ring precursor of ubiquinone: the contribution of At4g19010 significantly decreases when plants are switched from standard photoperiod to continuous high light intensities, while that of 4-CL8 and of the flavonoid pathway remains unchanged.

Biochemical Journal (2019) **476** 3521–3532
https://doi.org/10.1042/BCJ20190688

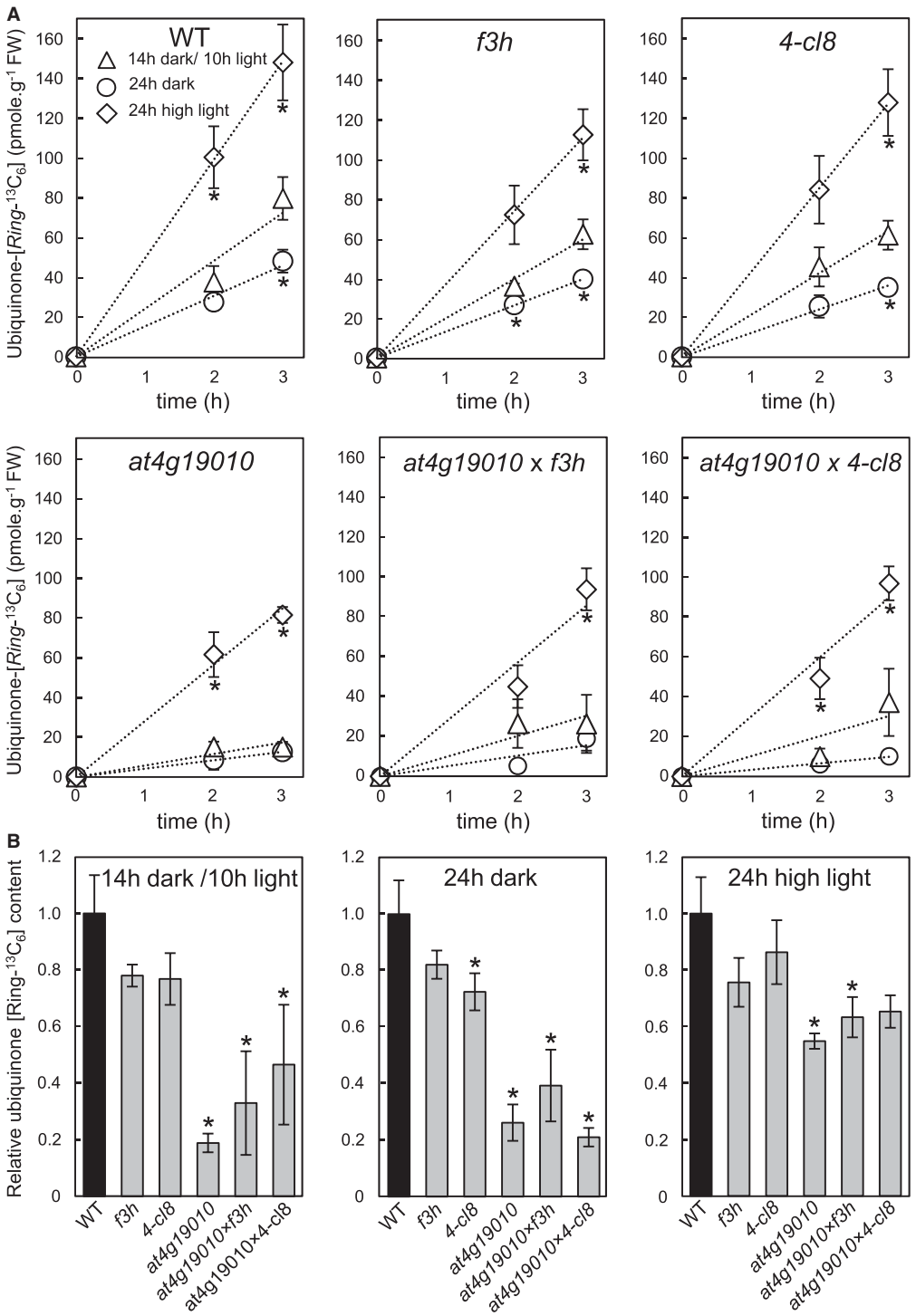

Figure 6. Effect of different light treatments on the *de novo* biosynthesis of ubiquinone from Phe in Arabidopsis.

(**a**) Ubiquinone-[*Ring*-$^{13}C_6$] levels in wild-type, *f3h*, *4-cl8*, *at4g19010*, *at4g19010* × *4cl8* and *at4g19010* × *f3h* axenic cultures fed for 2 and 3 h with 250 μM doses of Phe-[*Ring*-$^{13}C_6$]. Data are means of 3–6 biological replicates ± S.E. Asterisks indicate significant differences from the standard conditions (14 h-day) as determined by Fisher's test ($P < \alpha = 0.05$) from an analysis of variance. (**b**) Ubiquinone-[*Ring*-$^{13}C_6$] levels relative to wild-type controls after 3 h of feeding with 250 μM doses of Phe-[*Ring*-$^{13}C_6$]. Plants were subjected either to dark conditions or continuous high light (500 μE m^{-2} s^{-1}) for 24 h. Plants grown in standard conditions (14 h-day; 160 μE m^{-2} s^{-1}) served as controls. Data are means of 3–6 biological replicates ± S.E. Asterisks indicate significant differences from the wild-type control as determined by Fisher's test ($P < \alpha = 0.1$) from an analysis of variance.

PORTLAND PRESS

Biochemical Journal (2019) **476** 3521–3532
https://doi.org/10.1042/BCJ20190688

Discussion

Here we provide genetic and biochemical evidence that Arabidopsis possesses an additional *p*-coumaroyl-CoA ligase that participates in the biosynthesis of the ring precursor of ubiquinone in peroxisomes. This enzyme, product of gene *4-CL8* (*At5g38120*), is one of the eight members that make clade V of the acyl-activating enzyme superfamily in Arabidopsis [19,20]. *p*-Coumaroyl-CoA ligase At4g19010, which is also localized in peroxisomes and plays a central role in the β-oxidative conversion of *p*-coumarate into 4-hydroxybenzoate [10], belongs to the same clade [19,20]. Phylogenetic analyses indicate, however, that 4-CL8 and At4g19010 are not paralogous [19,20].

Although Clade V of acyl-activating enzymes appears to be conserved throughout land plant lineages, attributing cellular functions to its members has long been a vexing problem [19]. In fact, besides 4-CL8 and At4g1910, the only other clade V member of known physiological role is 3′-oxo-2-(2′-[Z]-pentenyl) cyclopentane-1-octanoic acid CoA ligase 1 (OPCL1) in the biosynthetic pathway of jasmonic acid [23]. Particularly puzzling to early studies of the phylogenetic relationships of this protein clade was that some of these enzymes were closely related to *p*-coumaroyl-CoA ligases involved in phenylpropanoid biosynthesis, which was known to take place in the cytosol, and yet displayed peroxisomal targeting sequence type I [19]. These observations were later reconciled by the finding that peroxisomes are actually able to import *p*-coumarate from the cytosol via the PXA1 transporter [10]. Along this line, that 4-CL8 is localized in peroxisomes while several of its top functional interactors detected in co-expression analysis encode for mitochondria-targeted proteins indicates that such a correlation is not merely attributable to a shared subcellular localization.

Our data show that the rate of ubiquinone biosynthesis from phenylalanine in Arabidopsis leaves more than doubles when plants are subjected to continuous high light treatments as compared with controls grown in standard conditions. This high light-driven increase in ubiquinone biosynthesis may reflect the roles that mitochondria play in support of photosynthesis, in particular with the oxidative decarboxylation and deamination of glycine originating from photorespiration and the export of tricarboxylic acid cycle intermediates for ammonia assimilation and amino acid biosynthesis [24–26]. Furthermore, it is thought that the respiratory chain participates in the re-oxidation of the excess of chloroplastic redox equivalents [24], and an increase in total dark respiration led by a larger input of electrons into the respiratory chain following high light treatments has indeed been reported [18]. Another reason, although non-exclusive with those just described, for the need of leaves to boost ubiquinone biosynthesis in response to high light exposure could be protection from photooxidative stress. Ubiquinone is a potent antioxidant, and its occurrence outside mitochondria is considered well established at least in animals and yeast [27–29]. The situation is less clear in plants [30], but the finding that high light exposure markedly stimulates ubiquinone biosynthesis calls for re-investigating the subcellular distribution of this prenylated quinone in plant tissues using the improved sensitivity and selectivity of current analytical methods.

That continuous high light treatments boosts the *de novo* biosynthesis of ubiquinone, together with the observation that such an increase is still present in the *f3h* mutant, where flavonol biosynthesis is blocked (Figure 6), indicate that in wild-type plants the strong demand for flavonol intermediates during anthocyanin production is unlikely to significantly compete for the usage of kaempferol as a precursor of ubiquinone. In other words, the biosynthetic flux of kaempferol is not the parameter that could explain the change in the rate of ubiquinone biosynthesis in response to continuous high light or dark treatments. This result could be explained in part by the fact that the quantity of kaempferol needed for ubiquinone biosynthesis is minute. For instance, calculations show that the pool size of 4-hydroxybenzoate originating from the peroxidative cleavage of kaempferol -i.e. directed towards ubiquinone biosynthesis- represents ∼ 0.1% of total kaempferol [11]. It results that, even if anthocyanin biosynthesis were to drain 99% of the pool of kaempferol, the latter would still occur at a 10-fold excess of the quantity required to fully sustain ubiquinone biosynthesis. Moreover, given that *in vivo* most of kaempferol is glycosylated on C-3 and that the cognate *o*-glycosyl esters are refractory to peroxidative cleavage [11], it is likely that it is the proportion of kaempferol aglycone that controls the biosynthetic flux of 4-hydroxybenzoate rather than the total pool size of kaempferol *per se*.

As concluding remarks, our data indicate that Arabidopsis 4-CL8 is involved in the β-oxidative metabolism of *p*-coumarate into 4-hydroxybenzoate in peroxisomes. The contribution of 4-CL8 to 4-hydroxybenzoate biosynthesis does not appear to significantly vary in response to light treatments. Both the biosynthesis of flavonol and 4-CL8 appear therefore to have housekeeping roles with respect to ubiquinone biosynthesis. In contrast, the contribution of At4g19010, which bears 70% to 80% of the biosynthetic flux of 4-hydroxybenzoate from

phenylalanine for ubiquinone production in standard photoperiod or in the dark, drops by about half in high light. This result points to the existence of either at least another ligase or an alternative pathway involved in the biosynthesis of the ring precursor of ubiquinone in plants.

Abbreviations

4-CL, 4-coumarate-CoA ligase; 4-HB, 4-hydroxybenzoate; C4H, cinnamate-4-hydroxylase; DMSO, dimethyl sulfoxide; F3H, flavanone-3-hydroxylase; FLS, flavonol synthase; FW, fresh weight; GFP, green fluorescent protein; HPLC, high performance liquid chromatography; KAT2, 3-keto-acyl-CoA thiolase 2; PAL, phenylalanine ammonia lyase; RFP, red fluorescent protein; RT-PCR, reverse transcriptase polymerase chain reaction.

Author Contribution

E.S., M.K., A.C.B., S.A.K, S.L., T.S.J., C.E., A.K.B., and G.J.B designed and performed the experiments, and analyzed the data. T.A.C. contributed to the experimental design, analyzed the data and contributed to the preparation of the manuscript. E.S., S.A.K and G.J.B. wrote the manuscript.

Funding

This work was made possible in part by National Science Foundation Grant MCB-1712608 (G.J.B.), and GRFP DGE-1842473 (A.C.B.), the USDA-ARS Floriculture and Nursery Research Initiative (T.A.C.), and the Plant Molecular and Cellular Biology Program (M. K.).

Competing Interests

The authors declare that there are no competing interests associated with the manuscript.

References

1 Turunen, M., Olsson, J. and Dallner, G. (2004) Metabolism and function of coenzyme Q. *Biochim. Biophys. Acta* **1660**, 171–199 https://doi.org/10.1016/j.bbamem.2003.11.012
2 Aussel, L., Pierrel, F., Loiseau, L., Lombard, M., Fontecave, M. and Barras, F. (2014) Biosynthesis and physiology of coenzyme Q in bacteria. *Biochim. Biophys. Acta* **1837**, 1004–1011 https://doi.org/10.1016/j.bbabio.2014.01.015
3 Schertl, P. and Braun, H.P. (2014) Respiratory electron transfer pathways in plant mitochondria. *Front. Plant Sci.* **5**, 163 https://doi.org/10.3389/fpls.2014.00163
4 Rasmusson, A.G., Soole, K.L. and Elthon, T.E. (2004) Alternative NAD(P)H dehydrogenases of plant mitochondria. *Annu. Rev. Plant Biol.* **55**, 23–39 https://doi.org/10.1146/annurev.arplant.55.031903.141720
5 Tsui, H.S., Pham, N.V.B., Amer, B.R., Bradley, M.C., Gosschalk, J.E., Gallagher-Jones, M. et al. (2019) Human COQ10A and COQ10B are distinct lipid-binding START domain proteins required for coenzyme Q function. *J. Lipid Res.* **60**, 1293–1310 https://doi.org/10.1194/jlr.M093534
6 Ohara, K., Kokado, Y., Yamamoto, H., Sato, F. and Yazaki, K. (2004) Engineering of ubiquinone biosynthesis using the yeast coq2 gene confers oxidative stress tolerance in transgenic tobacco. *Plant J.* **40**, 734–743 https://doi.org/10.1111/j.1365-313X.2004.02246.x
7 Liu, M., Chen, X., Wang, M. and Lu, S. (2019) SmPPT, a 4-hydroxybenzoate polyprenyl diphosphate transferase gene involved in ubiquinone biosynthesis, confers salt tolerance in *Salvia miltiorrhiza*. *Plant Cell Rep.* **38**, 1527–1540 https://doi.org/10.1007/s00299-019-02463-5
8 Okada, K., Ohara, K., Yazaki, K., Nozaki, K., Uchida, N., Kawamukai, M. et al. (2004) The AtPPT1 gene encoding 4-hydroxybenzoate polyprenyl diphosphate transferase in ubiquinone biosynthesis is required for embryo development in *Arabidopsis thaliana*. *Plant Mol. Biol.* **55**, 567–577 https://doi.org/10.1007/s11103-004-1298-4
9 Ducluzeau, A.L., Wamboldt, Y., Elowsky, C.G., Mackenzie, S.A., Schuurink, R.C. and Basset, G.J. (2012) Gene network reconstruction identifies the authentic trans-prenyl diphosphate synthase that makes the solanesyl moiety of ubiquinone-9 in Arabidopsis. *Plant J.* **69**, 366–375 https://doi.org/10.1111/j.1365-313X.2011.04796.x
10 Block, A., Widhalm, J.R., Fatihi, A., Cahoon, R.E., Wamboldt, Y., Elowsky, C. et al. (2014) The origin and biosynthesis of the benzenoid moiety of ubiquinone (Coenzyme Q) in *Arabidopsis*. *Plant Cell* **26**, 1938–1948 https://doi.org/10.1105/tpc.114.125807
11 Soubeyrand, E., Johnson, T.S., Latimer, S., Block, A., Kim, J., Colquhoun, T.A. et al. (2018) The peroxidative cleavage of kaempferol contributes to the biosynthesis of the benzenoid moiety of ubiquinone in plants. *Plant Cell* **30**, 2910–2921 https://doi.org/10.1105/tpc.18.00688
12 Dawson, R.M.C., Elliot, D.C., Elliot, W.H. and Jones, K.M. (1986) *Data for Biochemical Research*, Oxford University Press, New York
13 Alonso, J.M., Stepanova, A.N., Leisse, T.J., Kim, C.J., Chen, H., Shinn, P. et al. (2003) Genome-wide insertional mutagenesis of *Arabidopsis thaliana*. *Science* **301**, 653–657 https://doi.org/10.1126/science.1086391
14 Masini, L. (2014). *Investigation of the Molecular Basis of PAMP-Induced Resistance*. PhD thesis, University of East Anglia, The Sainsbury Laboratory, Norwich, U.K
15 Karimi, M., Inze, D. and Depicker, A. (2002) GATEWAY vectors for Agrobacterium-mediated plant transformation. *Trends Plant Sci.* **7**, 193–195 https://doi.org/10.1016/S1360-1385(02)02251-3
16 Clough, S.J. and Bent, A.F. (1998) Floral dip: a simplified method for Agrobacterium-mediated transformation of *arabidopsis thaliana*. *Plant J.* **16**, 735–743 https://doi.org/10.1046/j.1365-313x.1998.00343.x
17 Obayashi, T., Aoki, Y., Tadaka, S., Kagaya, Y. and Kinoshita, K. (2018) ATTED-II in 2018: a plant coexpression database based on investigation of the statistical property of the mutual rank index. *Plant Cell Physiol.* **59**, 440 https://doi.org/10.1093/pcp/pcx209

Biochemical Journal (2019) **476** 3521–3532
https://doi.org/10.1042/BCJ20190688

18 Wallström, S.V., Florez-Sarasa, I., Araújo, W.L., Escobar, M.A., Geisler, D.A., Aidemark, M. et al. (2014) Suppression of NDA-type alternative mitochondrial NAD(P)H dehydrogenases in *Arabidopsis thaliana* modifies growth and metabolism, but not high light stimulation of mitochondrial electron transport. *Plant Cell Physiol.* **55**, 881–896 https://doi.org/10.1093/pcp/pcu021

19 Shockey, J. and Browse, J. (2011) Genome-level and biochemical diversity of the acyl-activating enzyme superfamily in plants. *Plant J.* **66**, 143–160 https://doi.org/10.1111/j.1365-313X.2011.04512.x

20 Shockey, J.M., Fulda, M.S. and Browse, J. (2003) *Arabidopsis* contains a large superfamily of acyl-activating enzymes. Phylogenetic and biochemical analysis reveals a new class of acyl-coenzyme a synthetases. *Plant Physiol.* **132**, 1065–1076 https://doi.org/10.1104/pp.103.020552

21 Agati, G., Brunetti, C., Di Ferdinando, M., Ferrini, F., Pollastri, S. and Tattini, M. (2013) Functional roles of flavonoids in photoprotection: new evidence, lessons from the past. *Plant Physiol. Biochem.* **72**, 35–45 https://doi.org/10.1016/j.plaphy.2013.03.014

22 Saito, K., Yonekura-Sakakibara, K., Nakabayashi, R., Higashi, Y., Yamazaki, M., Tohge, T. et al. (2013) The flavonoid biosynthetic pathway in *Arabidopsis*: structural and genetic diversity. *Plant Physiol. Biochem.* **72**, 21–34 https://doi.org/10.1016/j.plaphy.2013.02.001

23 Koo, A.J., Chung, H.S., Kobayashi, Y. and Howe, G.A. (2006) Identification of a peroxisomal acyl-activating enzyme involved in the biosynthesis of jasmonic acid in *arabidopsis*. *J. Biol. Chem.* **281**, 33511–33520 https://doi.org/10.1074/jbc.M607854200

24 Krömer, S. (1995) Respiration during photosynthesis. *Annu. Rev. Plant Physiol. Plant Mol. Biol.* **46**, 45–70 https://doi.org/10.1146/annurev.pp.46.060195.000401

25 Raghavendra, A.S. and Padmasree, K. (2003) Beneficial interactions of mitochondrial metabolism with photosynthetic carbon assimilation. *Trends Plant Sci.* **8**, 546–553 https://doi.org/10.1016/j.tplants.2003.09.015

26 Douce, R., Bourguignon, J., Neuburger, M. and Rébeillé, F. (2001) The glycine decarboxylase system: a fascinating complex. *Trends Plant Sci.* **6**, 167–176 https://doi.org/10.1016/S1360-1385(01)01892-1

27 Seshadri sastry, P., Jayaraman, J. and Ramasarma, T. (1961) Distribution of coenzyme Q in rat liver cell fractions. *Nature* **189**, 577 https://doi.org/10.1038/189577a0

28 Bentinger, M., Tekle, M. and Dallner, G. (2010) Coenzyme Q-biosynthesis and functions. *Biochem. Biophys. Res. Commun.* **396**, 74–79 https://doi.org/10.1016/j.bbrc.2010.02.147

29 Awad, A.M., Bradley, M.C., Fernández-Del-Río, L., Nag, A., Tsui, H.S. and Clarke, C.F. (2018) Coenzyme Q(10) deficiencies: pathways in yeast and humans. *Essays Biochem.* **62**, 361–376 https://doi.org/10.1042/EBC20170106

30 Crane, F.L. (1959) Internal distribution of coenzyme Q in higher plants. *Plant Physiol.* **34**, 128–131 https://doi.org/10.1104/pp.34.2.128